Development of resiquimod-loaded modified PLA-based nanoparticles for cancer immunotherapy: A kinetic study

Cédric Thauvin[a], Jérôme Widmer[b], Inès Mottas[a,b], Sandra Hocevar[a], Eric Allémann[a], Carole Bourquin[a,b,c,*,1], Florence Delie[a,*,1]

[a] School of Pharmaceutical Sciences, University of Geneva, University of Lausanne, Rue Michel-Servet 1, 1211 Geneva, Switzerland
[b] Chair of Pharmacology, Faculty of Science and Medicine, University of Fribourg, Chemin du Musée 5, 1700 Fribourg, Switzerland
[c] Faculty of Medicine, University of Geneva, Rue Michel-Servet 1, 1211 Geneva, Switzerland

ARTICLE INFO

Keywords:
Modified PLA
Nanoparticles
Drug release
Immunostimulation
Resiquimod
TLR7 agonist
Microwave-assisted chemistry

ABSTRACT

Resiquimod (R848), a member of the imidazoquinoline family, is a Toll-like receptor 7/8 agonist with high potency for cancer immunotherapy. However, tolerance induction and adverse effects limit its development as a drug. Encapsulation in a polymer matrix can circumvent these limitations, as shown in our formerly published approach where R848 was loaded into polylactic acid (PLA)-based nanoparticles (NP). Although the results were encouraging, low rates of encapsulation and rapid release of the drug were observed. In this study, we present a new strategy using mixed NP from modified linear PLA in order to improve the encapsulation and modulate the release profile of R848. Modified PLA polymers were designed and synthesized by microwave-assisted ring opening polymerization of D,L-lactide, using polyethylene glycol as initiator to increase the hydrophilic properties of the polymer or linear saturated aliphatic chains (C8 or C20) to increase the affinity with hydrophobic R848. NP were prepared by solvent evaporation method, leading to particles of 205–288 nm loaded with either R848 or DiO as a tracking agent. The release profile showed longer retention of R848 at both neutral and acidic pH for NP from grafted polymers. Upon exposure to phagocytic immune cells, NP were actively taken up by the cells and no impact on cell viability was observed, independently of the constitutive polymer. All R848-loaded NP activated macrophages to secrete interleukin-6, demonstrating that the drug cargo was immunologically active. Importantly, macrophage activation by NP-delivered R848 was slower than with free R848, in accordance with the *in vitro* release profiles. Thus, NP prepared from modified PLA polymers showed no signs of toxicity to immune cells and efficiently delivered their immunoactive cargo in a delayed manner. This delivery strategy may enhance the efficacy and safety of small-molecule immunostimulants.

1. Introduction

Cancer immunotherapy is based on the reactivation of immunity against tumor tissues. During the initiation of an anticancer immune response, antigen-presenting cells (APC) take up tumor antigens within the tumor tissue to carry them to the lymph nodes. There, the APCs activate cytotoxic T cells, which migrate back to the tumor to kill the cancer cells [1]. Importantly, the APCs must themselves first be activated through their pattern-recognition receptors, in order to be fully functional. The Toll-like receptors (TLRs) are one of the main families of pattern-recognition receptors expressed by APCs, and their stimulation by endogenous or exogenous ligands leads to the production of proinflammatory cytokines [2]. Imidazoquinolines are a family of small-molecule immune response modifiers that stimulate specifically the TLRs 7 and 8 [3]. In this family, imiquimod and resiquimod (R848) are two low molecular weight and poorly water-soluble highly potent synthetic molecules with a very similar chemical structure. Imiquimod-based creams are approved for the treatment of different cutaneous malignant neoplasms after topical application [4–6]. Resiquimod has been described as a more potent inducer of cytokines in peripheral blood mononuclear cells [7,8]. Imidazoquinolines have been tested for the systemic treatment of non-skin cancers [9]. However, the outcome of these studies were quite disappointing, partly due to a phenomenon of TLR tolerance [10] and a poor bioavailability related to the poor

* Corresponding authors at: School of Pharmaceutical Sciences, University of Geneva, University of Lausanne, Rue Michel-Servet 1, 1211 Geneva, Switzerland (C. Bourquin and F. Delie).
E-mail addresses: carole.bourquin@unige.ch (C. Bourquin), florence.delie@unige.ch (F. Delie).
[1] The authors contributed equally to this work.

water solubility of the molecules. Furthermore, adverse effects such as leukopenia have also been described [11,12].

The use of nanoparticles (NP) made of polylactic acid (PLA) or poly (lactic-co-glycolic) acid (PLGA) to improve the biodistribution of hydrophobic active pharmaceutical ingredients (API) while reducing the possible side effects has been widely studied and proved efficient [13,14]. However, only a few publications, mainly published in the last two years, deal with the use of these NP loaded with immunomodulators for the promotion of an efficient *in vivo* immune response [15–18]. We recently showed that NP made of methoxy-polyethylene glycol PLA (mPEG-PLA) copolymers or a mixture of PLGA and mPEG-PLA copolymers represented a promising and safe delivery system to target resiquimod to lymph nodes [19]. We also showed that we were able to change PLA-based NP release kinetics, by chemically modifying the PLA polymers they are made with [20]. Among the main outcomes of these studies, it appeared necessary to improve the release kinetics of resiquimod with a better control of the burst effect and a prolongation of the release over time.

In his work dedicated to the synthesis and use of novel modified PLA copolymers, Michael Möller demonstrated that adding a hydrophobic pattern to the polymer backbone significantly changed the properties of the resulting polymeric micelles [21–24]. Indeed, starting from a monohexyl-substituted or dihexyl-substituted D,L-lactide, the syntheses of modified PLA polymers by ring opening polymerization (ROP) led to polyesters in which half or all monomer units were functionalized by a hexyl group. This change improved the drug loading capacity of the resulting drug delivery system (DDS) and drastically slowed down the release kinetics of various active ingredients.

In the present project, a deeper investigation of the impact of modified PLA on the loading of resiquimod and its release kinetic profile is presented. For this purpose, $mPEG_{2000}$, octanol or eicosanol were grafted to the PLA backbone while synthesizing 40 kDa polymers *via* microwave-assisted ROP of D,L lactide. We then prepared NP with PLA and modified PLA and compared their loading capacities and *in vitro* release kinetics. While hydrophilic $mPEG_{2000}$ was selected to increase the biodistribution of the NP suspension, the hydrophobic linear aliphatic chains were selected to enhance the hydrophobic characteristics of NP and therefore to improve encapsulation rate and extend the drug release profile. This study illustrates how the chemical modification of PLA can improve resiquimod loading in PLA-based NP. These NP were investigated to compare their biological activity on cell uptake and cytotoxicity as well as immune cell activation.

2. Material and methods

2.1. Materials for NP synthesis

D,L-lactide, stannous octoate ($Sn(Oct)_2$), 1,8-diazabicyclo(5.4.0) undec-7-ene (DBU), initiators (D,L-lactic acid, octanol, eicosanol and methoxy-poly(ethylene glycol) 2000 ($mPEG_{2000}$)), 3,3′Dioctadecyl-oxacarbocyanine perchlorate (DiO), polyvinyl alcohol (PVAL) (Mowiol 4–88, 26000 Da, 88% hydrolysis) and sucrose were purchased from Sigma-Aldrich (St. Louis, MO, USA). Resiquimod (R848) was purchased from Enzo Life Sciences. Chloroform ($CHCl_3$), dichloromethane (CH_2Cl_2), methanol (MeOH), hexane, tetrahydrofuran (THF) were purchased from Sigma-Aldrich (St. Louis, MO, USA). Phosphate-buffer saline (PBS) and fetal calf serum (FCS) were purchased from Gibco (Thermo Fisher Scientific, Inc., Waltham, MA, USA).

All materials were used as received without any further purification. Water was filtered through a Millipak 40 filter by a Millipore system.

2.2. Synthesis of PLA-based polymers

A solution of octanol or eicosanol (1 eq) as initiator, D,L-lactide (278 eq), and $Sn(Oct)_2$ as a catalyst (5 mol% relative to D,L-lactide) in $CHCl_3$ or a solution of lactic acid or $mPEG_{2000}$ (1 eq) as initiator, D,L-lactide (278 eq), and DBU as a catalyst (5 mol% relative to D,L-lactide) in $CHCl_3$ was irradiated in a microwave reactor (Biotage® Initiator+, Uppsala, Sweden) at 175 °C or at 125 °C for 5 min under nitrogen atmosphere. The resulting mixture was poured into HCl 0.1 M and extracted with CH_2Cl_2, washed with brine and water. Hexane was then added to the organic layer and the precipitate was centrifuged for 5 min at 3000*g*. After 3 cycles of dissolution of the pellet in a mixture of CH_2Cl_2/MeOH (8:2), precipitation in hexane and centrifugation for 5 min at 3000*g*, the resulting pellets were dried under reduced pressure to give PLA, PLA-C8, PLA-C20 and PLA-mPEG2000 as white solids in 60%, 35%, 23% and 83% yield, respectively.

2.3. Characterization of PLA-based polymers

The chemical structure and molecular composition of PLA-based polymers were determined by proton nuclear magnetic resonance (^1H NMR) spectroscopy in deuterated chloroform ($CDCl_3$) on a Varian Gemini 300 MHz NMR spectrometer (Palo Alto, CA, USA).

2.4. Preparation of nanoparticles

NP were prepared by emulsion solvent evaporation method as reported in Widmer et al. 2018 [19]. Briefly, 150 mg of polymers (the different ratios of PLA-based polymers are presented in Table 1) dissolved in 1 ml dichloromethane were emulsified in 2 ml of a 2.5% PVAL solution (w/v) by ultrasonication (Branson Ultrasonics, Danbury, USA) for 40 s and with an amplitude of 50% in an ice bath. The freshly prepared emulsion was then added dropwise to 50 ml of ultra-pure water and stirred 1 h at 1450 rpm with an Ultra-Turrax Eurostar digital Euros ST D (IKA-Werke GmbH & Co., Staufen, Germany) in an ice bath. The stirring speed was then reduced to 600 rpm and the solution was stirred for 2 h at room temperature to allow solvent evaporation. 3 cycles of washing and centrifugation using an Avanti 30 Centrifuge (Beckman, USA) equipped with a F1010 Fixed-Angle Rotor (Beckman, USA), each time for 20 min at 34000*g*, were finally necessary to obtain 10 ml of a pure suspension of NP. The latter was then divided in five fractions of 2 ml in which 1 ml of a 15% w/w sucrose aqueous solution was added as cryoprotectant. The samples were freeze dried using a Christ Alpha 2–4 LD plus freeze dryer (Christ, Osterode am Harz, Germany).

For loaded NP, either R848 (5 mg) or DiO (22.5 µg) were solubilized in dichloromethane and added to the polymer solution.

For R848-loaded NP, one fraction of 2 ml of pure suspension of NP was freeze-dried without additional sucrose in order to determine the drug loading.

Burst-free samples of R848-loaded NP were prepared for specific biological experiments to study the effect of the encapsulated fraction of R848. The R848-loaded NP were suspended in PBS supplemented with 10% (v/v) FCS for 40 min at 37 °C under a gentle shaking (80 rpm). One cycle of washing and centrifugation (20 min at 34000*g*), was applied to obtain 2 ml of a suspension of burst-free NP in which 1 ml of a 15% w/w sucrose aqueous solution was added before freeze-

Table 1
Composition of the different batches of PLA-based NP.

NP name	Polymer composition of NP (proportion w/w)				Loading
	$PLA\text{-}PEG_{2000}$	PLA	PLA-C8	PLA-C20	
u-NP	1/3	2/3	/	/	/
u-NP-C8	1/3	/	2/3	/	/
u-NP-C20	1/3	/	/	2/3	/
DiO-NP	1/3	2/3	/	/	DiO
DiO-NP-C8	1/3	/	2/3	/	DiO
R848-NP	1/3	2/3	/	/	R848
R848-NP-C8	1/3	/	2/3	/	R848
R848-NP-C20	1/3	/	/	2/3	R848

drying.

2.5. Nanoparticle characterization

2.5.1. Dynamic light scattering

NP size were determined before lyophilization by dynamic light scattering with a Zetasizer 3000 (Malvern Instruments, Ltd., U.K.) after dilution of nanoparticle suspensions in Milli-Q filtered water according to the supplier's recommendations: ca. 0.1 mg/ml to get a slightly opalescent suspension.

2.5.2. Scanning electron microscopy

NP morphology was determined by scanning electron microscopy (SEM) using a JSM-7001FA microscope (JEOL, Tokyo, Japan). A drop of aqueous suspension of NP was placed onto a carbon-coated stub, dried under vacuum and covered with a 15–20 nm layer of gold. The stubs were observed at an emission of 5.0 kV and a working distance of 9.3–12.0 nm. Pictures were taken for each sample at a magnification of 20000.

2.5.3. Drug loading

Samples of freeze-dried R848-loaded NP and freeze-dried burst-free R848-loaded NP (3 mg) were dissolved in HPLC grade DMSO (300 µl) and the loaded amount of R848 was quantified by a U-HPLC separation performed by a Thermo Scientific Accela LC system equipped with a Thermo Scientific Accela PDA (Thermo Fischer Scientific, Waltham, USA). The column used was a C18 Hypersil Gold (50x2.1 mm, 1.9 µm particle size, 175 Å pore size; Thermo Fischer Scientific, Waltham, USA). The chromatographic separation was carried out with a linear gradient mode starting from 2% acetonitrile and 98% of water containing 0.1% of formic acid (1.8–4 min) to 98% of acetonitrile containing 0.1% of formic acid (for 2 min) and 2% of water with a flow rate of 400 µl/min. R848 was detected at 320 nm wavelength. The injection volume was 10 µl. The peak of R848 was well separated in the chromatographic conditions established. The quantity of R848 was calculated by interpolation from the calibration curves. The calibration curves were linear within the 1.5–150 µg/ml range for R848, with a correlation coefficient (R^2) greater than 0.99. The method was adapted from Cruz et al. [25].

2.6. In vitro release kinetics

A suspension of 30 mg of freeze-dried R848-loaded NP in 10 ml PBS supplemented with 10% (v/v) FCS was split into vials containing 200 µl of the suspension and stirred at 80 rpm and 37 °C for different times (t0, 15 min, 30 min, 45 min, 1 h, 2 h, 3 h, 6 h, 12 h, 24 h, 48 h, 72 h, and 168 h), each in triplicate. At each time point, the suspensions were centrifuged at 16000*g* for 5 min (Avanti 30 centrifuge, Beckman, IN, USA) and the fluorescence of resiquimod in the supernatant was quantified by a U-HPLC separation with the same equipment as described above. The chromatographic separation was carried out with a linear gradient mode starting from 90% of water containing 0.1% of formic acid (1–4.5 min) to 98% of acetonitrile containing 0.1% of formic acid (4.5–6 min) with a flow rate of 400 µl/min. R848 was detected at 320 nm wavelength. The injection volume was 10 µl.

The same protocol was followed on suspension of freeze-dried burst-free R848-loaded NP either in PBS supplemented with 10% (v/v) FCS or in acetate buffer pH 4.5 for different times (t0, 30 min, 1 h, 2 h, 4 h, 6 h, 9 h, 12 h, 24 h, 48 h, 72 h, and 168 h).

2.7. Cell line

The murine macrophage cell line J774.1 (ATCC) was cultured in complete medium consisting of high glucose (4.5 g/l) DMEM (Biowest), 10% FCS (Biological industries), 2 mmol/ml L-glutamine (PAA), 1 mM sodium pyruvate (PAA), 1 IU/ml penicillin (PAA), and 100 µg/ml streptomycin (PAA). For experiments, cells were seeded in a flat-bottom 96-well plate at a concentration of 5×10^4 cell/ml (100 µl per well) and cultured overnight at 37 °C in 5% CO_2 before exposure to NP.

2.8. NP dilution

The NP concentrations selected for biological assays were based on R848 encapsulation values. Unloaded NP were used at the same concentration as the corresponding R848-loaded NP. Lyophilized NP were suspended in complete medium at 2 times the R848 working concentration (R848 working concentration: 0.1 µg/ml) and added to the cells in a 1:1 ratio.

2.9. NP uptake into cells

J774 cells were exposed for 3 h to DiO-labeled NP at 4 °C or 37 °C. Next, cells were washed in PBS and stained with Zombie Violet (Biolegend) to exclude dead cells. Live cells were analyzed for NP uptake and expressed as the percentage of DiO-positive cells.

Splenocytes were harvested from C57BL/6 mice (Janvier Labs) in accordance with Swiss regulations for animal experimentation. Briefly, spleens were cut in pieces, passed through a 70 µm strainer, and washed with PBS. Red blood cell lysis (BD Pharm Lyse, BD) was performed according to the manufacturer's instructions. Cells were resuspended in complete medium: RPMI1640 (PAA), 2 mol/l L-glutamine (PAA), 1 IU/ml penicillin (PAA), 100 µg/ml streptomycin (PAA), 0.1 mM non-essential amino acid (PAA), 1 mM sodium pyruvate (Life Technologies) and 25 µM betamercapto-ethanol (Life Technologies). Splenocytes (2×10^6 cells/ml in a 12-well plate) were incubated for 2 h with DiO-NP, harvested and washed twice with PBS. Cells were then incubated with FcX Block CD16/32 for 15 min prior to the addition of the following antibodies: CD11b (APC, clone M1/70), CD3 (Pacific Blue, clone 17A2), CD19 (APC-Cy7, 6D5) and CD11c (PE, clone N418), all from Biolegend. Immune cell subtypes were defined as follows: T lymphocytes (CD3+), B lymphocytes Monocytes/macrophages (CD11b+, CD11c-), dendritic cells (CD11b+, CD11c+). The different cell types were analyzed for NP uptake, expressed as the percentage of DiO-positive cells within that cell subtype.

2.10. Viability assay

J774 cells (5×10^4 cells in 100 µl/well) were exposed to NP for 24 h. Staurosporine (0.1 µM) was used as a positive control for cell death. Cells were stained with Annexin V in Annexin V buffer (Biolegend) to determine apoptotic cells. Zombie Violet staining (Biolegend) was used (diluted 1:1000 in PBS) as staining for dead cells. Flow cytometry analysis were performed by MACSquant analyzer 10 (Miltenyi Biotec).

2.11. Immune cell activation

J774 cells (5×10^4 cells in 100 µl/well) were exposed to NP for different times. The working concentration of all R848-NP conditions was 0.1 µg/ml. Free R848 was used as positive control (0.1 µg/ml). After incubation, supernatants were harvested and analyzed by ELISA MAX kit (Biolegend) for interleukin-6 (IL-6) according to the manufacturer's protocol. Absorbance was read by an Infinite 200 PRO plate reader (TECAN).

To assess the release of bioactive R848 from the NP, NP were incubated in complete medium (37 °C) for 1 h, 3 h, 6 h or 24 h without cells. NP were then centrifuged for 30 min at 12000*g* and supernatant was collected. NP supernatant was then added to J774 cells as a replacement of culture media. After 24 h, cell supernatant was collected and analyzed by ELISA for IL-6.

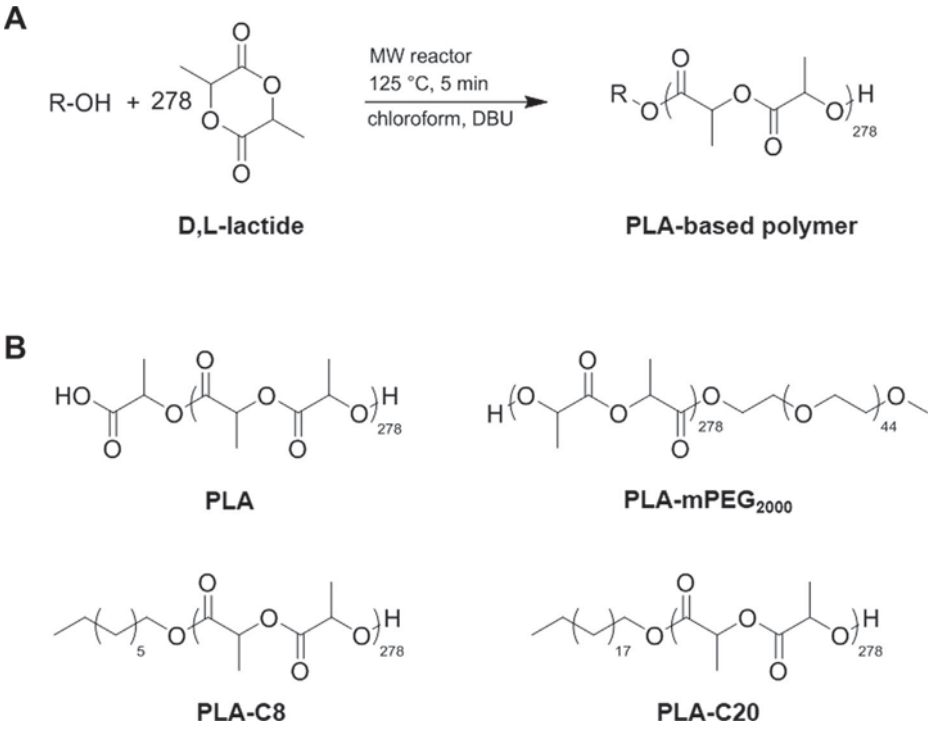

Fig. 1. General scheme of microwave-assisted ROP of D,L-lactide initiated by hydroxyl group bearing compounds (A) and chemical structure of the PLA-based polymers synthesized (B).

3. Results and discussion

3.1. Synthesis of PLA-based polymers

In this study, one non-modified "bare" PLA, named PLA thereafter, and three linear modified PLA were designed and synthesized *via* microwave-assisted ROP of D,L-lactide using different hydroxyl group bearing initiators (Fig. 1A). The use of microwave-assisted chemistry was preferred to classical thermal heating, due to its excellent temperature control, thereby preventing thermal decomposition or side reactions and leading to homogeneous batches of polymers [26]. On the one hand, PLA synthesis was initiated by D,L-lactic acid. On the other hand, modified PLA syntheses were either initiated by octanol or eicosanol, C8 and C20 linear saturated aliphatic alcohol, respectively, to graft hydrophobic properties to the polyester backbone, or $mPEG_{2000}$ to graft hydrophilic properties, to obtain PLA-C8, PLA-C20 and PLA-$mPEG_{2000}$, respectively (Fig. 1B). PLA was used as a reference. In order to be consistent with our previous work, and to allow a comparative study, we set the molecular weight of the four polymers at 40 kDa by using an accurate initiator to monomer ratio: 1 equivalent of initiator and 278 equivalents of D,L-lactide. Purity and molecular weight of the synthesized polymers were confirm by ^{1}H NMR spectroscopy by observing the absence of peaks corresponding to D,L-lactide and by integrating multiplets from PLA (5.17 ppm and 1.57 ppm) and singlet from mPEG (3.64 ppm), eicosanol or octanol (1.25 ppm), respectively (Supplementary Fig. S1). The analyses showed in all cases a total conversion of monomers into polymers and a final molecular weight, given as weight average, close to the predicted 40 kDa. All modified PLA were obtained as white solids with yields ranging from 23 to 35% when stannous octoate was used as catalyst and from 60 to 83% with DBU.

Among his research projects, Michael Möller focused on tuning the hydrophilic/lipophilic balance of PLA by developing mPEG-poly(monohexyl-substituted lactides) (mPEG-mHexPLA) or mPEG-poly(dihexyl-substituted lactides) (mPEG-diHexPLA). In contrast to our approach, the hydrophobicity was not provided by the initiator but by the substituted D,L-lactides. By varying the number of hexyl groups along the PLA chain, the increased loading abilities of micelles made from mPEG-mHexPLA or mPEG-diHexPLA have been clearly demonstrated with different hydrophobic compounds [21–24,27].

As we focused on the delivery of resiquimod for systemic administration, the main objective of this study was to obtain an adapted drug release. We demonstrated recently the interest of encapsulating R848 into derivatives of PLA-based NP to trigger an immune response [19]. However, these particles exhibited a fast burst release. Therefore, we decided to increase the hydrophobicity of the polymer to favor R848 retention while optimizing its release. Our aim was to prevent release of the cargo during the transport of the NP to the lymph nodes, in order to obtain only a local immune activation in the targeted lymphoid organs rather than a systemic activation. Such a systemic activation by small-molecule TLR7 agonists has been shown to be toxic [28]. Thus our linear modified PLA polymers, taking the example of a 40 kDa PLA, were grafted with only one C8 or C20 aliphatic chain to the polyester backbone instead of 139 and 278 C6 aliphatic side chains in case of mPEG-mHexPLA and mPEG-diHexPLA, respectively.

3.2. Preparation and characterization of PLA-based nanoparticles

Batches of NP made of PLA, PLA-C8 or PLA-C20 (2/3 w/w) and PLA-$mPEG_{2000}$ (1/3 w/w) were synthesized by a solvent evaporation method. These NP were either loaded with R848 as the active molecule (R848-NP and R848-NP-C8), loaded with DiO as a fluorescent probe (DiO-NP and DiO-NP-C8) or unloaded (u-NP, u-NP-C8 and u-NP-C20) (Table 2). Dynamic light scattering (DLS) analyses showed a monomodal distribution of size for all samples ranging from 205 to 288 nm with a general polydispersity index (PDI) lower than 0.18. Scanning electron microscopy (SEM) (Fig. 2) confirmed the spherical and homogeneous shape of NP as well as larger sizes in case of R848-loaded NP. Regarding the loading properties of the different NP, Table 2 shows that R848-NP was able to load five times more resiquimod than R848-NP-C8 and R848-NP-C20, although PLA-C8 or PLA-C20 polymers were specifically designed to improve hydrophobic interactions with the API thus resulting in an increased ability to load the API inside the

Table 2
Characterization of the NP batches.

NP	Mean size in intensity [nm]	PDI	µg R848/mg NP (entrapment efficiency [%])	
			R848-loaded NP	Burst-free R848-loaded NP
u-NP	217	0.14		
u-NP-C8	230	0.05		
u-NP-C20	257	0.05		
DiO-NP	205	0.18		
DiO-NP-C8	213	0.07		
R848-NP	282	0.13	12.03 (36)	3.12 (9)
R848-NP-C8	288	0.10	2.64 (8)	1.02 (3)
R848-NP-C20	282	0.09	2.66 (8)	1.08 (3)

corresponding NP. Steric hindrance might explain the lower loading efficiency due to the generation of a structural disorder in the final NP matrix. However, in case of burst-free R848-loaded NP the ability of NP made of PLA to load more resiquimod than NP made of modified PLA was still observed but this time with only a factor 3 giving a favorable result on the ability of modified PLA-based NP to better retain the API. We also did not observe significant difference between R848-loaded NP made of C8-modified polymers or C20-modified polymers.

3.3. *In vitro release kinetics*

To evaluate the influence of PLA structural changes on drug release, we investigated the *in vitro* release kinetics of the three types of R848-loaded NP (Fig. 3). This assay was first carried out on samples of freeze-dried R848-loaded NP in PBS pH 7.4 supplemented with 10% v/v FCS at 37 °C, over a period of seven days and maintaining sink conditions. This aqueous medium was used to mimic the biological environment that would be encountered during the diffusion towards the target cells. A 100% release of R848 corresponds to the maximum amount of drug contained in NP and determined by the drug loading assays.

Fig. 3A shows that the burst release, equivalent to the rapid desorption of drug from the NP surface, was similar in all cases with more than 15% of resiquimod released in the first 15 min. This observation might be the consequence of a similar external structure of the R848-loaded NP. Indeed, all NP types are composed of 1/3 w/w of PLA-mPEG$_{2000}$ copolymer whose hydrophilic moieties are mainly located in the outer shell of the resulting NP. The burst release phase was then followed by the controlled release phase which corresponds to the release of the drug due to diffusion through the DDS matrix or degradation of the DDS matrix and depends on the nature of the interactions

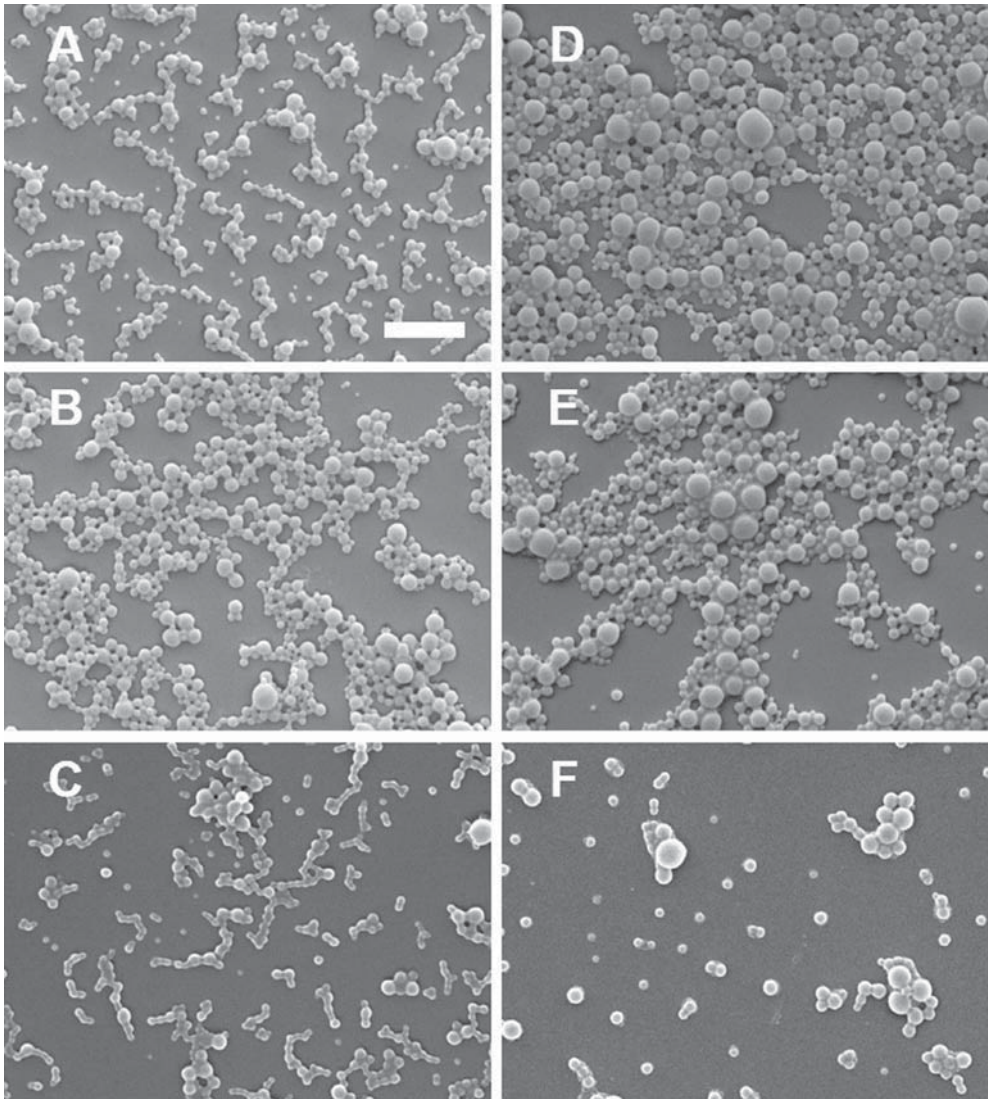

Fig. 2. Scanning electron microscopy images of unloaded (u-NP-C20 (A), u-NP-C8 (B) and u-NP (C)) and R848-loaded NP (R848-NP-C20 (D), R848-NP-C8 (E) and R848-NP (F)) (scale bar = 1 µm).

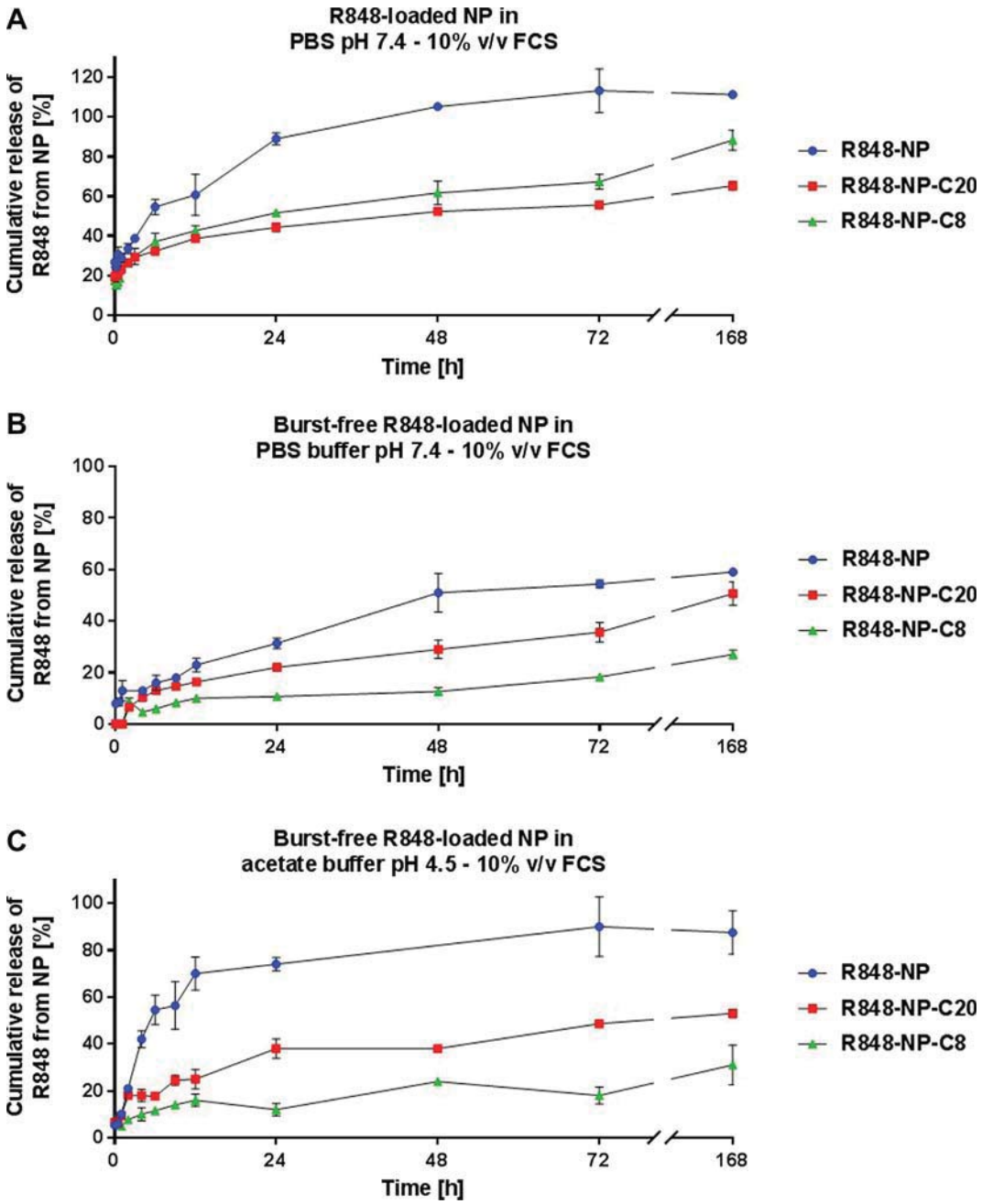

Fig. 3. In vitro release profiles of R848 from R848-loaded NP in PBS pH 7.4 supplemented with 10% v/v FCS (A), and from burst-free R848-loaded NP in PBS pH 7.4 supplemented with 10% v/v FCS (B) and in acetate buffer pH 4.5 (C), over a period of 168 h at 37 °C. Each value represents mean ± SD, n = 3.

between the API and the DDS [29]. In the case of R848-NP, this diffusion-dependent release reached a cumulative amount of resiquimod of 100% after 48 h followed by a plateau. For R848-NP-C8 and R848-NP-C20, 62% and 52% of resiquimod were released after 48 h. This was followed by another phase corresponding to a slower release of the API to finally reach a cumulative amount of resiquimod of 88% and 65% for R848-NP-C8 and R848-NP-C20, respectively, from 48 h to 168 h. The trend observed in this kinetic study suggests that R848-NP-C8 and R848-NP-C20 retain resiquimod better than R848-NP, which is consistent with our expectations. No differences were observed between R848-NP-C8 and R848-NP-C20.

A burst effect was observed with the first set of samples. Burst-free R848-loaded NP were therefore produced by suspending R848-loaded NP in PBS buffer at 37 °C for 40 min under gentle stirring to eliminate the fraction of R848 which was weakly incorporated in the outer shell of NP. In vitro release kinetics were then carried out on these samples either in PBS pH 7.4 supplemented with 10% v/v FCS or in acetate buffer pH 4.5. Acetate buffer was selected to mimic the acidic milieu of the endosome of APCs where the TLR7, target of R848, is located [30]. The burst effect considerably decreased when PBS/FCS was used (Fig. 3B) as less than 15% of resiquimod were released after 1 h. No release was observed with burst-free R848-NP-C8 and burst-free R848-NP-C20 over the same period. Then, a rapid release phase was observed over a period of 48 h for burst-free R848-NP to reach a cumulative amount of resiquimod of 51%. This rapid release was observed after only 12 h with burst-free R848-NP-C8 and burst-free R848-NP-C20, to reach a cumulative amount of resiquimod of 12% and 16%, respectively. Finally, a slower release phase was observed to reach 59%, 27% and 51% of resiquimod released from burst-free R848-NP, burst-free R848-NP-C8 and burst-free R848-NP-C20, respectively, from 24 h to

168 h. In acetate buffer (Fig. 3C), we also observed a lower burst effect as less than 10% of resiquimod were released after 1 h in all cases. Then, cumulative amounts of resiquimod of 74%, 12% and 38% after 24 h were observed with burst-free R848-NP, burst-free R848-NP-C8 and burst-free R848-NP-C20, respectively. It was followed by a slower release of API to finally reach a cumulative amount of resiquimod of 88%, 31% and 53% for burst-free R848-NP, burst-free R848-NP-C8 and burst-free R848-NP-C20, respectively, from 24 h to 168 h.

Both *in vitro* release profiles of R848 from burst-free R848-loaded NP in PBS pH 7.4 supplemented with 10% v/v FCS and in acetate buffer pH 4.5 showed a better retention of the API by modified PLA-based NP. This observation was even more evident in acetate buffer as more than 50% of resiquimod was released after 6 h with PLA-based NP *vs* less than 20% with modified PLA-based NP, thereby proving the interest of adding hydrophobic chains on the PLA backbone.

3.4. Uptake of PLA-NP by immune cells

We then examined how the PLA-based NP interact with cells of the immune system. Macrophages and dendritic cells are immune cells specialized in the uptake and processing of particulate material. To assess whether the PLA-based NP were taken up by these cells, we exposed a macrophage cell line, J774, to NP or NP-C8 labeled with the fluorescent marker DiO at 4 °C or 37 °C. Cells were then analyzed by flow cytometry and the percentage of DiO-positive cells was determined. Both types of NP were efficiently taken up by the macrophages at 37 °C, with approximately 70% of cells labeled with DiO after 3 h independently of the polymer. Low temperature reduces endocytosis activity [31], and the incubation at 4 °C consequently showed a lower proportion of DIO-positive cells, at around 50% for DiO-NP and 20% for DiO-NP-C8 (Fig. 4A and B). It is possible that in the absence of active internalization processes at low temperatures, the DiO-labeled particles were not internalized by the cells at 4 °C but rather adhered to the cell surface.

To examine whether the PLA-based NP were also taken up by primary immune cells rather than a cell line, freshly isolated mouse splenocytes were exposed to fluorescently labeled NP for 2 h at 37 °C. Mouse splenocytes are composed of many different immune cells types, which can be easily distinguished by flow cytometry. We observed that DiO-NP and DiO-NP-C8 were mainly taken up by macrophages after this short incubation time. In contrast, T and B lymphocytes as well as dendritic cells showed few DiO-positive cells (Fig. 4C). Thus, highly phagocytic cells such as macrophages actively take up different PLA NP.

3.5. Impact of PLA-NP on macrophage viability

In view of a future biomedical application of NP as a drug-loaded carrier, it is essential to determine whether the NP show any cytotoxic activity on immune cells. We exposed J774 macrophages to different types of NP loaded or not with R848 or to free R848 for 24 h and measured cell viability by flow cytometry. The NP concentration was selected to deliver a pharmacologically active concentration of R848 (0.1 μg/ml). Staurosporine was used as positive control. Importantly, NP had no significant impact on cell viability in this experimental setting, independently of the presence of their drug cargo (Fig. 5). These results demonstrate that the PLA-NP do not impair the viability of immune cells even at NP concentrations of at least 8 μg/ml.

3.6. Impact of PLA-NP on macrophage function

R848 is an immune-activating drug that binds to the Toll-like receptor 7 in the endosome of dendritic cells and macrophages. TLR7 activation leads to the production and secretion of pro-inflammatory cytokines, such as interleukin-6 (IL-6) [32]. To determine whether the R848 cargo of the NP could lead to immune activation, we measured the secretion of IL-6 into the supernatant by J774 macrophages exposed to different types of PLA NP loaded with R848. We show that all R848-loaded NP induced production of IL-6 by the macrophages after 24 h in culture, and that the level of cytokines released was similar to the level induced by free R848 (Fig. 6). Only slight differences were seen in the levels of IL-6 released by exposure to R848-loaded NP with different chemical modifications of PLA. Importantly, NP without R848 cargo (u-NP-C8, u-NP-C20) did not induce any IL-6 release, indicating that the NP material alone does not have an immunostimulatory effect. We obtained similar findings for TNFα (Supplementary Fig. S2). We did not detect secretion of IL-1β after exposure of J774 cells to either R848-loaded or unloaded NP (data not shown).

Since we had shown that the release of R848 differs between the different types of PLA-NP at early time points (Fig. 3), we examined the impact of exposure of J774 macrophages to R848-loaded NP for shorter incubation times. We found that R848-NP, R848-NP-C8 and R848-NP-C20 all led to lower production of IL-6 by macrophages at 6 and 8 h incubation, compared to the same amount of free R848 (Fig. 7A). The difference was no longer detected after 12 h incubation. This is in line with the data presented in Fig. 3 showing a controlled release of R848 by the NP.

To investigate how the different release kinetics of R848 from the NP affect cell stimulation over time, we incubated burst-free NP in cell culture medium at 37 °C for 1 to 24 h, collected the NP supernatant and exposed J774 macrophages to the supernatant for 24 h. We then again measured IL-6 production by macrophages. Supernatants harvested after a 1-h incubation with all types of NP did not lead to IL-6 production, supporting that R848 had not yet been released from the NP (Fig. 7B). Supernatants harvested after a 3-h incubation of burst-free

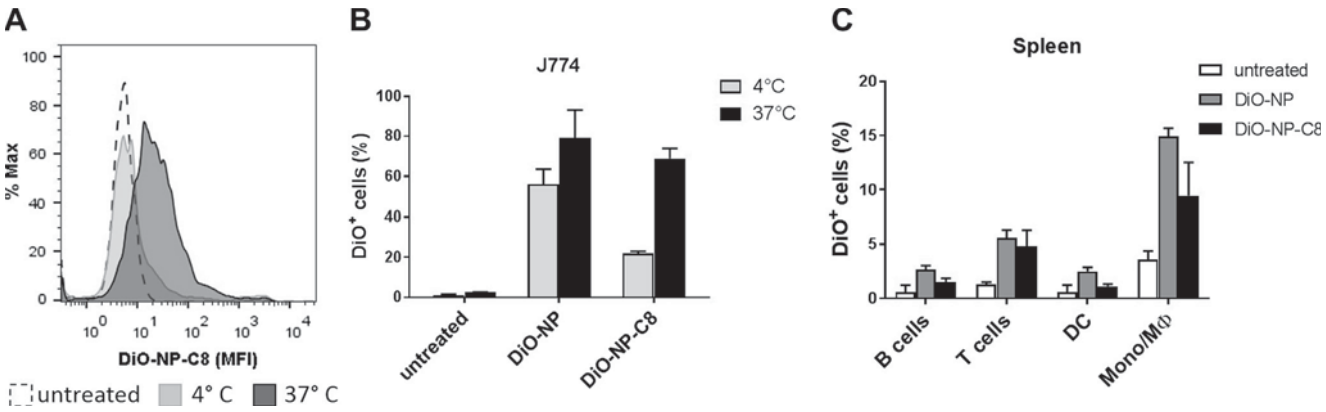

Fig. 4. NP are effectively taken up by antigen-presenting cells. Representative histogram (MFI) (A) and percentage of DiO-positive cells (B) after J774 macrophages were incubated with DiO-labeled NP for 3 h at 4 °C or 37 °C and assessed by flow cytometry. Freshly isolated mouse splenocytes were incubated with DiO-labeled NP at 37 °C for 2 h (C). Each bar represents mean ± SD, n = 3. Data are representative of two separate experiments.

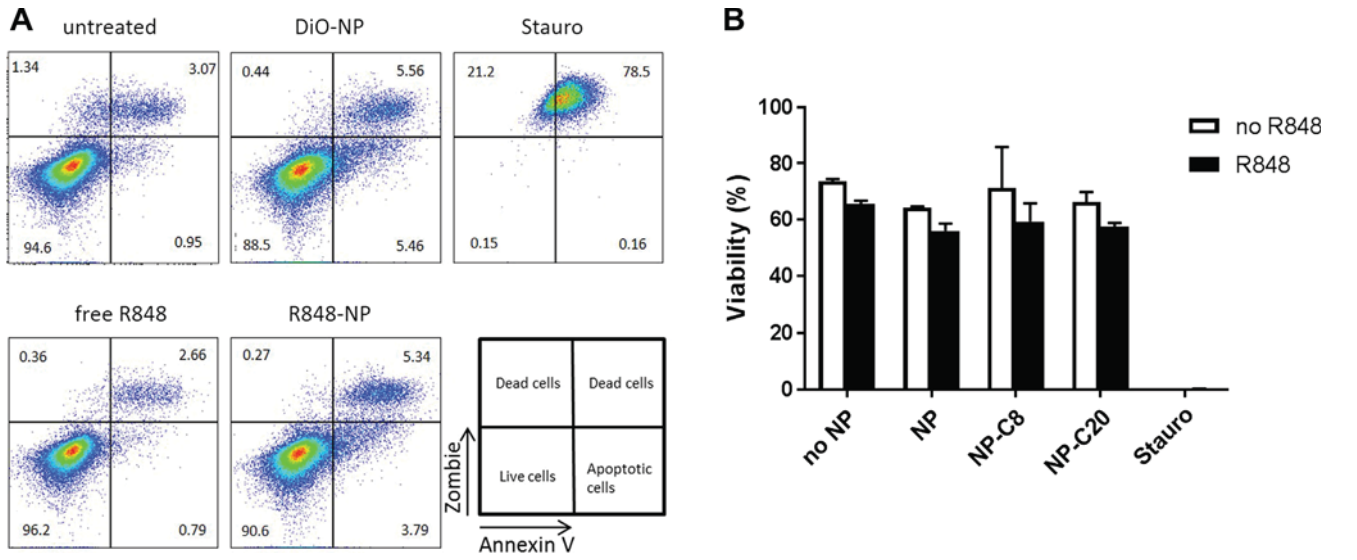

Fig. 5. PLA-NP do not impair macrophage viability. J774 cells were exposed for 24 h to different NP formulations (R848 concentration: 0.1 μg/ml for free R848 and all R848-loaded NP conditions). Representative flow cytometry dot plots (A) and percentage of live cells (B). Each bar represents mean ± SD, n = 3. Data are representative of three separate experiments. Stauro: staurosporine.

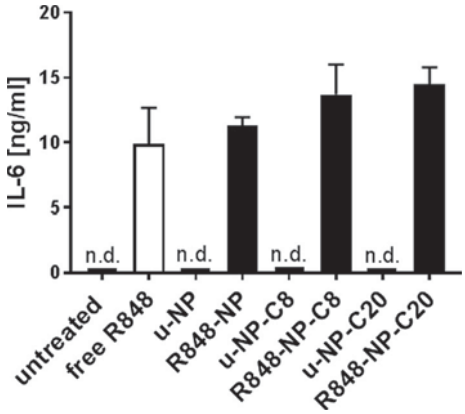

Fig. 6. R848-loaded PLA-NP activate cytokine release in macrophages. The release of IL-6 from J774 cells was assessed after incubation for 24 h with unloaded or R848-loaded NP (R848 concentration: 0.1 μg/ml for free R848 and all R848-loaded NP conditions). Each bar represents mean ± SD, n = 4. Data show one representative experiment out of four. n.d.: not detected.

R848-NP and burst-free R848-NP-C8 induced similar levels of IL-6, whereas supernatants from burst-free NP-R848-C20 did not induce IL-6 production at this time point. This suggests that R848 had not been released from the NP burst-free NP-R848-C20 after 3 h. No difference was seen between the different supernatants harvested after 6 h. Interestingly, the IL-6 production was higher for cells exposed to the supernatant of burst-free NP-R848-C20 harvested after 24 h, compared to supernatants from the other NP types. Overall, R848-loaded NP showed delayed activation of the cells in the first 8 h of incubation, compared to free R848.

4. Conclusion

In this study, one bare PLA and three linear modified PLA (PLA-mPEG$_{2000}$, PLA-C8 and PLA-C20) were successfully synthesized using microwave-assisted ROP of D,L-lactide. While PLA-mPEG$_{2000}$ was synthesized to improve the biodistribution of the resulting NP, PLA-C8 and PLA-C20 were used to increase the affinity with poorly water-soluble R848. NP were then prepared by mixing PLA-mPEG2000 (1/3 w/w) and PLA, PLA-C8 or PLA-C20 (2/3 w/w). Despite the changes made since our previous work [20], encapsulation efficiency of resiquimod remained low. Importantly, the use of PLA-C8 and PLA-C20 delayed the release of R848, especially in acidic conditions. Burst issues observed with R848-loaded NP were solved by preparing burst-free NP. Studies with phagocytic immune cells demonstrated that the addition of aliphatic chains to the PLA backbone did not impair cellular uptake and safety of the NP on macrophages. Moreover, all drug-loaded NP efficiently stimulated macrophages with a time lag in agreement with the matrix effect on drug release, showing the R848 cargo retained its

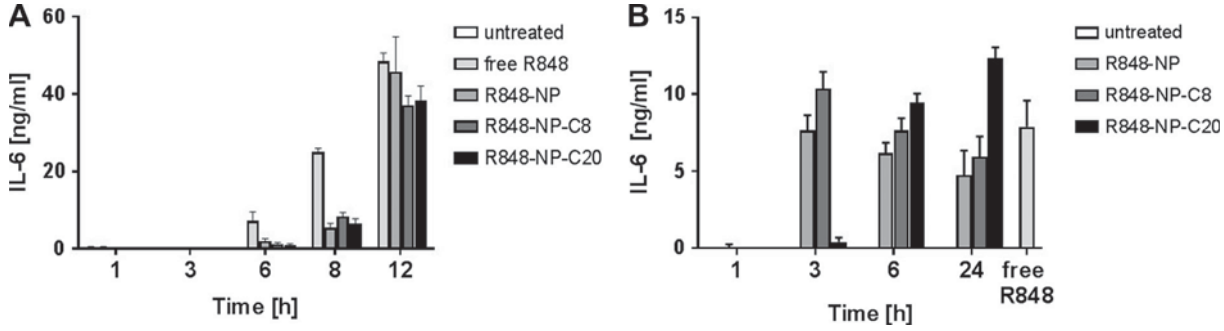

Fig. 7. R848-loaded NP activate macrophages more slowly than the free drug. IL-6 cytokine release after J774 cells exposure to R848-loaded NP or free R848 at different time points (A). IL-6 secretion by J774 cells after 24 h exposure to NP supernatant collected at different time points (1–24 h) (B). Each bar represents mean ± SD, n = 4. Data are representative of at least 2 separate experiments.

immunostimulatory function. In future studies, release profiles could further be optimized by using intrinsic properties of PLA and so by adapting its molecular weight or the size of the resulting NP. Thus, modification of PLA polymers in NP preparation allows to control the release kinetics for a small molecule immune response modifier. A stepwise and individualized optimization is necessary to obtain selected release characteristics.

Acknowledgments

The authors would like to acknowledge Mrs. Brigitte Delavy and Mrs. Nathalie Boulens for their contribution to the preparation and characterization of NP and for SEM analyses, respectively. This study was supported by the National Center of Competence in Research (NCCR) for Bio-Inspired Materials, the Swiss Cancer Research Foundation grant KFS4535-08-2018 and the Swiss National Science Foundation grants 156871, 156372 and 182317 to CB.

Conflict of interest

The authors declare no conflicts of interest.

Appendix A. Supplementary material

Supplementary data to this article can be found online

References

[1] D.S. Chen, I. Mellman, Oncology meets immunology: the cancer-immunity cycle, Immunity 39 (2013) 1–10, https://doi.org/10.1016/j.immuni.2013.07.012.

[2] M. Smith, E. Garcia-Martinez, M.R. Pitter, J. Fucikova, R. Spisek, L. Zitvogel, G. Kroemer, L. Galluzzi, Trial watch: toll-like receptor agonists in cancer immunotherapy, Oncoimmunology 7 (2018) e1526250, , https://doi.org/10.1080/2162402X.2018.1526250.

[3] M.P. Schon, M. Schon, TLR7 and TLR8 as targets in cancer therapy, Oncogene 27 (2008) 190–199, https://doi.org/10.1038/sj.onc.1210913.

[4] L. Edwards, A. Ferenczy, L. Eron, D. Baker, M.L. Owens, T.L. Fox, A.J. Hougham, K.A. Schmitt, Self-administered topical 5% imiquimod cream for external anogenital warts. HPV Study Group. Human PapillomaVirus, Arch. Dermatol. 134 (1998) 25–30, https://doi.org/10.1001/archderm.134.1.25.

[5] H. Kanzler, F.J. Barrat, E.M. Hessel, R.L. Coffman, Therapeutic targeting of innate immunity with toll-like receptor agonists and antagonists, Nat. Med. 13 (2007) 552–559, https://doi.org/10.1038/nm1589.

[6] K. Peris, E. Campione, T. Micantonio, G.C. Marulli, M.C. Fargnoli, S. Chimenti, Imiquimod treatment of superficial and nodular basal cell carcinoma: 12-week open-label trial, Dermatol Surg 31 (2005) 318–323, https://doi.org/10.1111/j.1524-4725.2005.31081.

[7] M. Kwissa, H.I. Nakaya, H. Oluoch, B. Pulendran, Distinct TLR adjuvants differentially stimulate systemic and local innate immune responses in nonhuman primates, Blood 119 (2012) 2044–2055, https://doi.org/10.1182/blood-2011-10-388579.

[8] T. Meyer, C. Surber, L.E. French, E. Stockfleth, Resiquimod, a topical drug for viral skin lesions and skin cancer, Expert Opin. Invest. Drugs 22 (2013) 149–159, https://doi.org/10.1517/13543784.2013.749236.

[9] B.J. Weigel, S. Cooley, T. DeFor, D.J. Weisdorf, A. Panoskaltsis-Mortari, W. Chen, B.R. Blazar, J.S. Miller, Prolonged subcutaneous administration of 852A, a novel systemic toll-like receptor 7 agonist, to activate innate immune responses in patients with advanced hematologic malignancies, Am. J. Hematol. 87 (2012) 953–956, https://doi.org/10.1002/ajh.23280.

[10] C. Bourquin, C. Hotz, D. Noerenberg, A. Voelkl, S. Heidegger, L.C. Roetzer, B. Storch, N. Sandholzer, C. Wurzenberger, D. Anz, S. Endres, Systemic cancer therapy with a small molecule agonist of toll-like receptor 7 can be improved by circumventing TLR tolerance, Cancer Res. 71 (2011) 5123–5133, https://doi.org/10.1158/0008-5472.

[11] P.J. Pockros, D. Guyader, H. Patton, M.J. Tong, T. Wright, J.G. McHutchison, T.C. Meng, Oral resiquimod in chronic HCV infection: safety and efficacy in 2 placebo-controlled, double-blind phase IIa studies, J. Hepatol. 47 (2007) 174–182, https://doi.org/10.1016/j.jhep.2007.02.025.

[12] M. Gunzer, H. Riemann, Y. Basoglu, A. Hillmer, C. Weishaupt, S. Balkow, B. Benninghoff, B. Ernst, M. Steinert, T. Scholzen, C. Sunderkotter, S. Grabbe, Systemic administration of a TLR7 ligand leads to transient immune incompetence due to peripheral-blood leukocyte depletion, Blood 106 (2005) 2424–2432, https://doi.org/10.1182/blood-2005-01-0342.

[13] J.I. Hare, T. Lammers, M.B. Ashford, S. Puri, G. Storm, S.T. Barry, Challenges and strategies in anti-cancer nanomedicine development: an industry perspective, Adv. Drug. Deliv. Rev. 108 (2017) 25–38, https://doi.org/10.1016/j.addr.2016.04.025.

[14] W. Song, S.N. Musetti, L. Huang, Nanomaterials for cancer immunotherapy, Biomaterials 148 (2017) 16–30, https://doi.org/10.1016/j.biomaterials.2017.09.017.

[15] Y. Dolen, M. Kreutz, U. Gileadi, J. Tel, A. Vasaturo, E.A. van Dinther, M.A. van Hout-Kuijer, V. Cerundolo, C.G. Figdor, Co-delivery of PLGA encapsulated invariant NKT cell agonist with antigenic protein induce strong T cell-mediated antitumor immune responses, Oncoimmunology 5 (2016) e1068493, , https://doi.org/10.1080/2162402X.2015.1068493.

[16] M. Ebrahimian, M. Hashemi, M. Maleki, G. Hashemitabar, K. Abnous, M. Ramezani, A. Haghparast, Co-delivery of dual toll-like receptor agonists and antigen in poly (lactic-co-glycolic) acid/polyethylenimine cationic hybrid nanoparticles promote efficient in vivo immune responses, Front. Immunol. 8 (2017) 1077, https://doi.org/10.3389/fimmu.2017.01077.

[17] D. Schmid, C.G. Park, C.A. Hartl, N. Subedi, A.N. Cartwright, R.B. Puerto, Y. Zheng, J. Maiarana, G.J. Freeman, K.W. Wucherpfennig, D.J. Irvine, M.S. Goldberg, T cell-targeting nanoparticles focus delivery of immunotherapy to improve antitumor immunity, Nat. Commun. 8 (2017) 1747, https://doi.org/10.1038/s41467-017-01830-8.

[18] I. Mottas, A. Bekdemir, A. Cereghetti, L. Spagnuolo, Y.S. Yang, M. Muller, D.J. Irvine, F. Stellacci, C. Bourquin, Amphiphilic nanoparticle delivery enhances the anticancer efficacy of a TLR7 ligand via local immune activation, Biomaterials 190–191 (2019) 111–120, https://doi.org/10.1016/j.biomaterials.2018.10.031.

[19] J. Widmer, C. Thauvin, I. Mottas, V.N. Nguyen, F. Delie, E. Allemann, C. Bourquin, Polymer-based nanoparticles loaded with a TLR7 ligand to target the lymph node for immunostimulation, Int. J. Pharm. 535 (2018) 444–451, https://doi.org/10.1016/j.ijpharm.2017.11.031.

[20] C. Thauvin, B. Schwarz, F. Delie, E. Allemann, Functionalized PLA polymers to control loading and/or release properties of drug-loaded nanoparticles, Int. J. Pharm. 548 (2018) 771–777, https://doi.org/10.1016/j.ijpharm.2017.11.001.

[21] Y.G. Bachhav, K. Mondon, Y.N. Kalia, R. Gurny, M. Moller, Novel micelle formulations to increase cutaneous bioavailability of azole antifungals, J. Control Release 153 (2011) 126–132, https://doi.org/10.1016/j.jconrel.2011.03.003.

[22] K. Mondon, M. Zeisser-Labouebe, R. Gurny, M. Moller, Novel cyclosporin A formulations using MPEG-hexyl-substituted polylactide micelles: a suitability study, Eur. J. Pharm. Biopharm. 77 (2011) 56–65, https://doi.org/10.1016/j.ejpb.2010.09.012.

[23] K. Mondon, M. Zeisser-Labouebe, R. Gurny, M. Moller, MPEG-hexPLA micelles as novel carriers for hypericin, a fluorescent marker for use in cancer diagnostics, Photochem. Photobiol. 87 (2011) 399–407, https://doi.org/10.1111/j.1751-1097.2010.00879.x.

[24] T. Trimaille, K. Mondon, R. Gurny, M. Moller, Novel polymeric micelles for hydrophobic drug delivery based on biodegradable poly(hexyl-substituted lactides), Int. J. Pharm. 319 (2006) 147–154, https://doi.org/10.1016/j.ijpharm.2006.03.036.

[25] L.J. Cruz, P.J. Tacken, F. Rueda, J.C. Domingo, F. Albericio, C.G. Figdor, Targeting nanoparticles to dendritic cells for immunotherapy, Methods Enzymol. 509 (2012) 143–163, https://doi.org/10.1016/B978-0-12-391858-1.00008-3.

[26] R. Hoogenboom, U.S. Schubert, Microwave-assisted polymer synthesis: recent developments in a rapidly expanding field of research, Macromol. Rapid Commun. 28 (2007) 368–386, https://doi.org/10.1002/marc.200600749.

[27] M. Lapteva, M. Mignot, K. Mondon, M. Moller, R. Gurny, Y.N. Kalia, Self-assembled mPEG-hexPLA polymeric nanocarriers for the targeted cutaneous delivery of imiquimod, Eur J Pharm Biopharm (2019), https://doi.org/10.1016/j.ejpb.2019.01.008 (in this issue).

[28] C. Bourquin, A. Pommier, C. Hotz, Harnessing the immune system to fight cancer with toll-like receptor and RIG-I-like receptor agonists, Pharmacol. Res. (2019), https://doi.org/10.1016/j.phrs.2019.03.001 in press.

[29] K.S. Soppimath, T.M. Aminabhavi, A.R. Kulkarni, W.E. Rudzinski, Biodegradable polymeric nanoparticles as drug delivery devices, J. Control Release 70 (2001) 1–20, https://doi.org/10.1016/S0168-3659(00)00339-4.

[30] Y. Hu, Z. Zhao, M. Ehrich, K. Fuhrman, C. Zhang, In vitro controlled release of antigen in dendritic cells using pH-sensitive liposome-polymeric hybrid nanoparticles, Polymer (Guildf) 80 (2015) 171–179, https://doi.org/10.1016/j.polymer.2015.10.048.

[31] V. Sokolova, D. Kozlova, T. Knuschke, J. Buer, A.M. Westendorf, M. Epple, Mechanism of the uptake of cationic and anionic calcium phosphate nanoparticles by cells, Acta Biomater 9 (2013) 7527–7535, https://doi.org/10.1016/j.actbio.2013.02.034.

[32] S.J. Gibson, J.M. Lindh, T.R. Riter, R.M. Gleason, L.M. Rogers, A.E. Fuller, J.L. Oesterich, K.B. Gorden, X. Qiu, S.W. McKane, R.J. Noelle, R.L. Miller, R.M. Kedl, P. Fitzgerald-Bocarsly, M.A. Tomai, J.P. Vasilakos, Plasmacytoid dendritic cells produce cytokines and mature in response to the TLR7 agonists, imiquimod and resiquimod, Cell Immunol. 218 (2002) 74–86, https://doi.org/10.1016/S0008-8749(02)00517-8.